# Gas Sorption, Diffusion and Permeation in Nafion®

Mohsin Mukaddam, Eric Litwiller, and Ingo Pinnau*

Advanced Membranes and Porous Materials Center (AMPMC), Physical Sciences and Engineering Division, Chemical and Biological Engineering Program, King Abdullah University of Science and Technology (KAUST), Al-Jazri Building 4, Thuwal, 23955-6900, Saudi Arabia

**Key words:** Nafion®, gas solubility, diffusion, permeability, selectivity, hydrocarbons

**ABSTRACT**

The gas permeability of dry Nafion® films was determined at 2 atm and 35 °C for He, $H_2$, $N_2$, $O_2$, $CO_2$, $CH_4$, $C_2H_6$ and $C_3H_8$. In addition, gas sorption isotherms were determined by gravimetric and barometric techniques as a function of pressure up to 20 atm. Nafion® exhibited linear sorption uptake for low-solubility gases, following Henry's law, and convex behavior for highly sorbing condensable gases, indicating rubber-like behavior at 35 °C. XRD results demonstrated that Nafion® contains bimodal amorphous chain domains with average d-spacing values of 2.3 and 5.3 Å. Only helium and hydrogen showed relatively high gas permeability of 37 and 7 Barrer, respectively; all other gases exhibited low permeability that decreased significantly as penetrant size increased. Dry Nafion® was characterized by extraordinarily high selectivities: $He/H_2$ = 5.2, $He/CH_4$ = 445, $He/C_2H_6$ = 1275, $He/C_3H_8$ = 7400, $CO_2/CH_4$ = 28, $CO_2/C_2H_6$ = 79, $CO_2/C_3H_8$ = 460, $H_2/CH_4$ = 84, $H_2/C_2H_6$ = 241, and $H_2/C_3H_8$ = 1400. These high selectivities could make Nafion® a potential candidate membrane material for dry feeds for helium recovery and carbon dioxide separation from natural gas and removal of higher hydrocarbons from hydrogen-containing refinery gases.

## INTRODUCTION

Separation processes account for ~45% of all process energy used in chemical and petroleum refining industries.[1] As the drive for energy savings and sustainability intensifies, more efficient separation technology becomes increasingly important. Membrane-based technology offers potential advantages over traditional processes such as cryogenic distillation and amine absorption in terms of cost, simplicity, size, and energy efficiency.[2,3] Commercial applications using membranes include onsite nitrogen production from air, hydrogen recovery from various refinery and petrochemical process streams, dehydration of air and carbon dioxide removal from natural gas.[4-8] Glassy polymers currently used for gas separations (polysulfone, cellulose acetate, polyimide) are limited in their commercial application spectrum due to their moderate permeability and selectivity and limited resistance to penetrant-induced plasticization. For feeds containing condensable components (such as $CO_2$, water vapor, $C_{3+}$ hydrocarbons, aromatics etc.) membrane plasticization often leads to highly undesirable loss in mixed-gas selectivity.[4,7,8,9-13]

An emerging materials class that can potentially mitigate some limitations of commercial gas separation membranes is based on perfluorinated solution-processable glassy polymers, including Teflon AF® (Du Pont), Hyflon® AD (Solvay), Cytop® (Asahi Glass) and others.[14-19] These polymers are known for their excellent chemical and thermal properties as a result of their strong C-F bond energy (485 kJ/mole) in comparison to C-C (360 kJ/mole) bonds in hydrocarbon polymers.[19] Their unique structure/gas transport property relationships have set the limits of permeability-selectivity combinations on the 2008 Robeson upper bound for certain gas pairs such as He/$CH_4$, He/$H_2$, $N_2$/$CH_4$, and $H_2$/$CH_4$.[20] Because of their high selectivities and chemical inertness, these polymers were proposed for gas separation applications, specifically

natural gas treatment, where condensable species were detrimental to the performance of traditional polymers as a result of plasticization.[14-16]

Another important class of perfluorinated polymers is based on sulfonated ionomers. Nafion® (Du Pont), the prototypical perfluorinated ionomer, has been the benchmark material in the fuel cell industry for several decades owing to its high proton conductivity and good chemical and thermal stability.[21,22] The structure of dry Nafion® consists of a hydrophobic perfluorocarbon backbone and a highly hydrophilic sulfonic acid tail (Figure 1a), which forms a dispersed phase of ionic clusters with diameters of 1.5 nm in the perfluorocarbon matrix (Figure 1b).[22-25] Surprisingly, only very limited pure-gas transport data have been reported for Nafion®.[26-31] The first comprehensive study on the gas permeation properties of dry Nafion® was reported by Chiou and Paul using the constant volume/variable pressure technique.[29] The gas diffusion coefficients were then deduced from the time-lag method. Their study indicated low permeability in dry Nafion® for all gases other than He and $H_2$. Recently, Fan et al. reported gas permeability measurements in dry Nafion® at different temperatures using the same technique.[30] Sarti's group evaluated the effects of temperature and relative humidity on Nafion® transport and found up to 100-fold increases in gas permeability relative to the values obtained under dry test conditions.[31,32]

The physical state of dry Nafion® (glass or rubber) has been under debate because of the significantly varying glass transition temperature values reported by several researchers.[22,25,33] As Nafion® consists of a phase-separated structure, it is expected to have two glass transition temperatures; one that represents the rubbery PTFE phase and another one induced by the ionic sulfonic acid clusters. Osborn et al. performed a comprehensive study on the glass transition of Nafion® using dynamic mechanical analysis (DMA) and concluded that the β transition observed

at -20 °C in Nafion® $H^+$ is the glass transition temperature of the rubbery phase in Nafion®.[33] This transition results from fluorocarbon main-chain motions within the framework of a *static* physically cross-linked network.[33]

Chiou and Paul showed that the $CO_2$ permeability increased with pressure, a typical behavior observed in rubbers, and suggested that this could possibly indicate that the rubbery phase dominates gas transport.[29] It was concluded that *direct* gas sorption measurements are necessary to gain more definitive insight into the role of the rubbery phase and the ionic cluster domains with respect to gas permeation in Nafion®. To date, to the best of our knowledge, only one study has reported directly measured gas sorption isotherms in Nafion®, and was limited to He and $H_2$.[34]

In this work, comprehensive data on the pure-gas permeability of He, $H_2$, $N_2$, $O_2$, $CO_2$, $CH_4$, $C_2H_6$, and $C_3H_8$ in Nafion® are reported. Additionally, extensive high-pressure gas sorption studies were performed using barometric and gravimetric sorption techniques at 35 °C. Diffusion coefficients were deduced using the solution-diffusion model and the directly measured permeability and solubility coefficients.

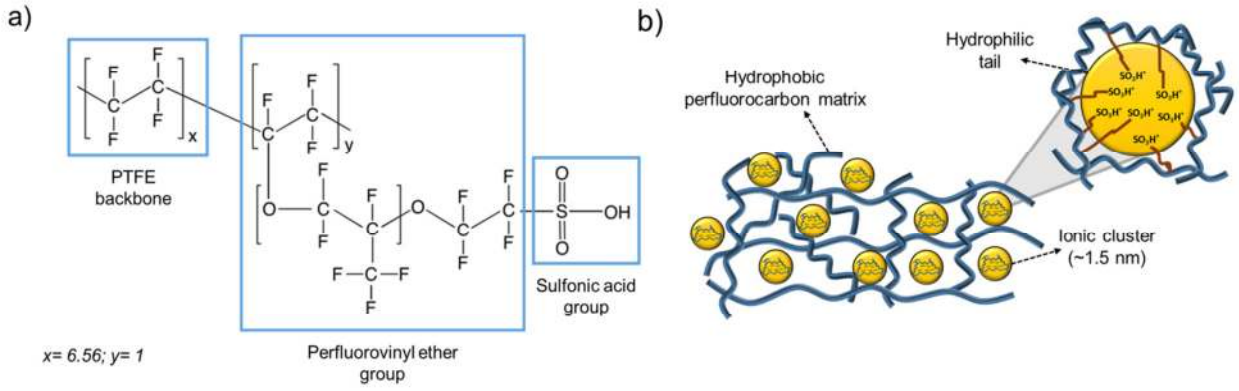

**Figure 1.** (a) Chemical structure of Nafion® (sulfonic acid form); x=6.56, y=1; (b) Cluster-network model for dry Nafion®.

## BACKGROUND AND THEORY

***Gas Permeability*.** The permeation of gases and vapors through a non-porous membrane is generally described by the solution-diffusion model.[35,36] The steady-state gas permeability through a membrane of thickness *l* is defined by:

$$P = \frac{N \cdot l}{p_{up} - p_{down}} \tag{1}$$

where *P* is the gas permeability coefficient ($cm^3$(STP)·cm/$cm^2$·s·cmHg), *N* is the steady-state gas flux ($cm^3$(STP)/$cm^2$·s) through the membrane, and $p_{up}$ and $p_{down}$ are the upstream and downstream pressure at the membrane interface, respectively.

The flux through the membrane is given by the following expression:

$$N = -D \cdot \frac{dC}{dx} \tag{2}$$

where *D* ($cm^2$/s) is the effective diffusion coefficient in the polymer, and *C* ($cm^3$(STP)/$cm^3$(polymer)) is the penetrant concentration in the membrane. Combining eq 1 and 2 and integrating across the membrane thickness gives:

$$P = D_{eff} \frac{C_{up} - C_{down}}{p_{up} - p_{down}} \tag{3}$$

where $D_{eff}$ is the concentration-averaged effective diffusion coefficient, and $C_{up}$ and $C_{down}$ are the penetrant concentration at the upstream and downstream side of the membrane, respectively. When the downstream pressure is much lower than the upstream pressure, eq 3 can be simplified:

$$P = D_{eff} \cdot \frac{C_{up}}{p_{up}} = D_{eff} \cdot S \tag{4}$$

where *S* is the solubility coefficient at the upstream side of the membrane.

***Gas Solubility in Polymers***

*Solubility in Rubbery Polymers*. Solubility of sparingly soluble gases in rubbery polymers or phase-separated macromolecules, like Nafion®, where the continuous fluorocarbon phase is rubbery, is characterized by a linear isotherm in which the gas concentration in the polymer obeys Henry's Law: $C = K_D \cdot p$, where $K_D$ is the Henry's constant and $p$ is the gas pressure.[36-38] However, for strongly sorbing gases (at high penetrant activity), the sorbed concentration deviates from ideal Henry's law behavior. In this case, the isotherm is convex to the pressure axis and the curvature depends upon the level of gas interaction with the polymer matrix. The magnitude of the polymer-penetrant interaction can then be expressed using the Flory-Huggins equation:

$$\ln a = \ln \Phi + (1 - \Phi) + \chi(1 - \Phi)^2 \quad (5)$$

where $a$ is the penetrant activity, $\Phi$ is the volume fraction occupied by the sorbed penetrant molecule, and $\chi$ is the Flory-Huggins interaction parameter. The penetrant activity is expressed as $p/p_{sat}$, where $p_{sat}$ is penetrant saturation vapor pressure at the temperature of the sorption experiment.

*Solubility in Glassy Polymers*. Gas sorption in glassy polymers differs markedly from that in rubbery polymers. The sorbed gas concentration shows a characteristic concave behavior at low pressure and is linear at high pressure. Such isotherms are most commonly described by the dual-mode sorption model, according to which initial gas sorption occurs in the non-equilibrium excess free volume portion of the polymer matrix generally referred to as the 'Langmuir sites' or

'holes'.[39,40] At a given temperature, a fixed number of holes are available, randomly distributed within the polymer matrix. Upon hole saturation, gas molecules then dissolve in the equilibrium dense portion of the polymer matrix – referred to as the 'Henry's mode' or 'dissolved mode' of sorption. The cumulative sorption occurring in the Langmuir holes and Henry's mode is mathematically represented as:

$$C = K_D \cdot p + \left(\frac{C'_H \cdot b \cdot p}{1 + b \cdot p}\right) \quad (6)$$

where $C'_H$ is the Langmuir saturation capacity parameter that describes the non-equilibrium excess free volume features of the glassy state, and $b$ characterizes the affinity between the penetrant and the Langmuir sites. Gas solubility is generally higher in glassy polymers than in rubbers due to this excess free volume.

***Gas Solubility Correlations*.** The solubility of gases depends on the relative affinity between gas and polymer, but more strongly on penetrant condensability – correlated with the gas critical temperature ($T_c$) or normal boiling point ($T_b$).[36,41] The relationship between solubility and penetrant condensability is generally expressed as:

$$\ln S = a + b \cdot T_c \quad (7)$$

The constant '$a$' is a measure of the overall sorption capacity and slope '$b$' represents the increase in solubility with penetrant condensability. The solubility of all common gases in hydrocarbon polymers (rubbery and glassy) generally obeys the trend described in eq 7 with $b$ values in the range of 0.017 – 0.019 $K^{-1}$.[36] However, deviations from the trend are seen for hydrocarbon gas solubility in perfluorocarbon polymers, as a result of unfavorable thermodynamic interactions.[16] Gas solubility in perfluorocarbon polymers is lower than in hydrocarbon-based polymers and the slope values range from 0.009 – 0.011 $K^{-1}$.[16]

## EXPERIMENTAL

***Materials.*** Isotropic Nafion® NRE 211 dispersion-cast films were obtained from Ion Power, Inc. in the $H^+$ form. These ion-exchange membranes had nominal thickness of 25 μm and equivalent weight of 1100 g $equiv^{-1}$. Because Nafion® tends to sorb water readily from the atmosphere, films were always dried at 80 °C under vacuum for 2 days prior to any measurements. Film density was determined using mass-volumetric and non-solvent buoyancy techniques and was equal to 2.01g/cc ± 0.014, which is consistent with previously reported density values for dry Nafion®.[42] The pure gases He, $H_2$, $N_2$, $O_2$, $CO_2$, $CH_4$, $C_2H_6$, $C_3H_8$, and *n*-$C_4H_{10}$ were purchased from Abdullah Hashim Group (AHG), KSA with purity of at least 99.99%.

***Wide Angle X-Ray Diffraction (WAXD).*** Wide angle x-ray measurements were conducted on a Bruker D8 Advance diffractometer using a Cu Kα X-ray source of characteristic wavelength λ = 1.54 Å with a step size of 0.05° for 5 s/step from 11 to 50°. Samples were pre-dried under vacuum at 80 °C for 2 days. The diffraction pattern was corrected for background scattering and the crystalline/amorphous peaks were fit to the Pearson VII distribution function with correlation coefficients greater than 99%. The relative crystallinity was calculated by integrating the area under the crystalline peak and dividing by the sum of the fitted integrated peak using the following equation:

$$x_c = \frac{\int_0^\infty I_{cr}\,(2\theta)d(2\theta)}{\int_0^\infty I_{cr}\,(2\theta)d(2\theta)+\int_0^\infty I_{am}\,(2\theta)d(2\theta)} \tag{9}$$

where $x_c$ is the fraction of crystallinity in the polymer, $I_{cr}$, $I_{am}$ are the sum of the intensities of the fitted crystalline and amorphous peaks, respectively, and 2θ is the diffraction angle.

***Gas Permeation Experiments.*** The pure-gas permeability of Nafion® was determined by using the constant volume/variable pressure method.[43,44] After drying the polymer film sample under vacuum at 80 °C for 2 days, it was partially masked with an impermeable aluminum tape such that the area available for gas transport was 5.0 $cm^2$. The sample was then mounted in the permeation system and exposed to vacuum from both upstream and downstream sides for at least 24 hours at 35 °C to degas the film. Pure-gas permeability of He, $H_2$, $N_2$, $O_2$, $CO_2$, $CH_4$, $C_2H_6$, and $C_3H_8$ was determined at 2 atm and 35 °C and calculated as follows:

$$P = D \cdot S = 10^{10} \frac{V_d \; l}{P_{up} \; ART} \frac{dp}{dt} \tag{10}$$

where $P$ is the permeability in Barrers (1 Barrer = $10^{-10}$ $cm^3$(STP)·cm/$cm^2$·s·cmHg), $p_{up}$ is the upstream pressure (cmHg), $dp/dt$ is the steady- state permeate-side pressure increase (cmHg/s), $V_d$ is the calibrated permeate volume ($cm^3$), $l$ is the membrane thickness (cm), $A$ is the effective membrane area ($cm^2$), $T$ is the operating temperature (K), and $R$ is the gas constant (0.278 $cm^3$·cmHg /$cm^3$(STP)·K). The ideal selectivity for a gas pair is given by the following relationship:

$$\alpha_{A/B} = \frac{P_A}{P_B} = \frac{D_A}{D_B} \; x \; \frac{S_A}{S_B} \tag{11}$$

The apparent diffusion coefficient $D$ ($cm^2$/s) was calculated from individual measurements of $P$ and $S$ ($cm^3$(STP)/$cm^3$·cmHg) by the relationship: $D=P/S$, in which the $S$ values were determined from the barometric sorption technique.

***Barometric Gas Sorption.*** High-pressure gas sorption of Nafion® was carried out using a custom-built dual-volume pressure decay apparatus based on an original design described

elsewhere.[45] Gas sorption isotherms were determined in the order: He, $H_2$, $N_2$, $O_2$, $CH_4$, $CO_2$, $C_2H_6$, $C_3H_8$ and *n*-$C_4H_{10}$. All measurements were performed at 35 °C up to pressures of 20 atm (except for $C_3H_8$ ~ 7 atm and *n*-$C_4H_{10}$ ~ 2 atm). After drying the polymer film sample (~ 1.5 g) in a vacuum oven at 80 °C for 2 days, a sample was placed in a sample holder and allowed to outgas under high vacuum over a period of 12 h at 35 °C. After introducing a gas at a desired pressure into the system, the decay in pressure with time due to gas sorption was continuously recorded with a data acquisition system using LabVIEW software (National Instruments) until the sample chamber pressure was constant. The amount of gas sorbed into the polymer was determined by mass balance. Thereafter, additional gas was introduced into the system to increase the pressure for the next measurement. This process was repeated until a complete isotherm was measured for a given gas as a function of pressure. The sample was then degassed under high vacuum for up to 5 days. To ensure that the sample reverted to its initial physical state after each gas was tested, one $N_2$ measurement was then repeated. Finally, the system was degassed again and the next gas was introduced into the system.

***Gravimetric Gas Sorption***. Gas solubility in Nafion® $H^+$ was also measured using a Hiden Intelligent Gravimetric Analyzer (IGA-003, Hiden Isochema, UK), which measures gas isotherms up to 20 atm. After drying a polymer film sample (~ 100 mg) in a vacuum oven at 80 °C for 2 days, it was mounted in the sorption apparatus and degassed under high vacuum ($< 10^{-7}$ mbar) at 35 °C until stable sample weight readings were obtained before beginning collection of the isotherm points. Then, gas was introduced in the sample chamber by a stepwise pressure ramp of 100 mbar/min until a desired pressure was reached. After equilibrium weight uptake was recorded, the next pressure point was set and this process was continued until the complete

isotherm was determined. After the measurement, the sample was degassed as described for the barometric method and all other gas sorption isotherms were determined in consecutive order.

## RESULTS AND DISCUSSION

***Microstructure of Nafion®.*** The chain packing in Nafion® can be qualitatively assessed with the WAXD spectrum presented in Figure 2. The spectrum indicates semi-crystalline behavior of Nafion® represented by the crystalline peak at $2\theta = 17.7°$ and two amorphous halo peaks at $2\theta = 16.8$ and $39.3°$ consistent with previously reported data.[46-49] The relative crystallinity calculated by fitting the crystalline and amorphous peaks from Figure 2 is 11.4%. These results agree with previously reported WAXD data for Nafion® with crystallinity values ranging between 12-22%.[22,48] Nafion® shows a bimodal amorphous distribution comprising regions with average chain d-spacings of 2.3 Å and 5.3 Å calculated from Bragg's equation, ($d = \lambda/2\sin\theta$). The region of very tight chain packing in Nafion® (average d-spacing ~2.3 Å over a wide diffraction angle range of 30-50°) is a consequence of several diffraction peaks from intermolecular correlations.[47] This observation has significant implications for the ability of Nafion® to selectively permeate helium ($d_k = 2.6$ Å) over all other gases, including hydrogen ($d_k = 2.89$ Å).

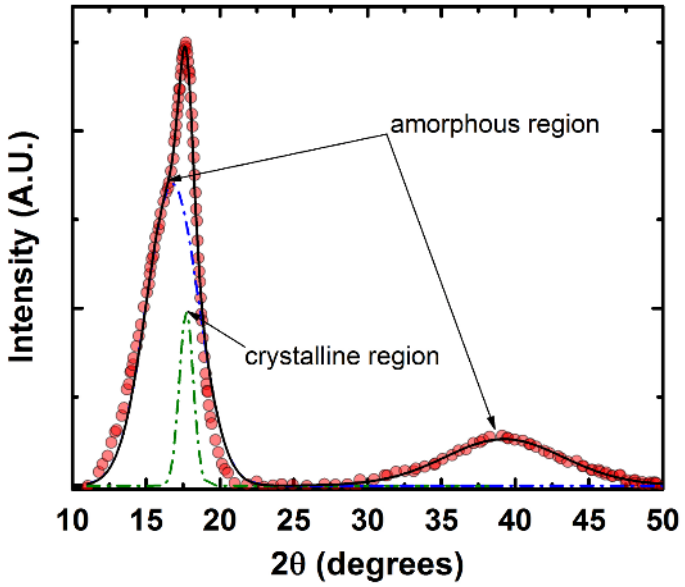


**Figure 2.** WAXD profile of Nafion® dried under vacuum at 80 °C for 2 days. The diffraction spectrum was corrected for background scattering and the crystalline and amorphous peaks were obtained by applying the Pearson VII distribution function on the original convoluted peak (red symbols). The black smooth line is the sum of crystalline and amorphous regions in the polymer.

***Pure-Gas Permeability***. The pure-gas permeation properties of He, $H_2$, $N_2$, $O_2$, $CO_2$, $CH_4$, $C_2H_6$ and $C_3H_8$ in Nafion® are presented in Table 1. The gas permeabilities follow the order of kinetic diameters ($d_k$): He > $H_2$ > $CO_2$ > $O_2$ > $N_2$ > $CH_4$ > $C_2H_6$ > $C_3H_8$ indicative of the strongly size-dependent permeation mechanism in Nafion®. The gas permeabilities at 35 °C reported in this study are in reasonably good agreement with those reported by Chiou and Paul.[29] However, the values reported by Fan et al. at 30 °C are approximately 20-40% lower than those reported here.[30] Possible reasons for this difference include: (i) Different film drying protocol; (ii) different permeation test conditions. In our study, the same film drying and permeation test protocol was applied for each film, which minimized possible errors due to sample variations.

**Table 1. Gas Permeability in Dry Nafion® at 2 atm and 35 °C.**

| Gas | Permeability (Barrer) | | |
|---|---|---|---|
| | This study | [29][a] | [30][b] |
| He | 37 | 41 | 29 |
| $H_2$ | 7 | 9.3 | 5.2 |
| $O_2$ | 1.01 | 1.08 | 0.72 |
| $N_2$ | 0.24 | 0.26 | 0.18 |
| $CO_2$ | 2.3 | 2.4 | 1.4 |
| $CH_4$ | 0.083 | 0.102 | 0.08 |
| $C_2H_6$ | 0.029 | - | - |
| $C_3H_8$ | 0.005 | - | - |

[a] 1 atm and 35 °C.[29]

[b] 4 atm and 30 °C.[30]

The permeability properties of Nafion® and rubbery polydimethylsiloxane (PDMS)[50], as a function of critical volume for several gases, are compared in Figure 3. In Nafion®, the permeability decreases significantly as the sizes of the gas molecules increase as is typically observed for low free volume glassy polymers. $C_2H_6$ and $C_3H_8$ exhibited *very* low permeability owing to their large size (low diffusivity) and commonly ascribed unfavorable hydrocarbon-fluorocarbon interaction (low gas solubility).[16] On the other hand, highly flexible rubbery PDMS shows markedly different permeation behavior: more condensable gases with large molecular size such as $C_2H_6$ and $C_3H_8$ exhibit higher permeability than smaller gases such as He and $H_2$.[50] In fact, PDMS shows about 6 orders of magnitude higher $C_3H_8$ permeability than Nafion®. This behaviour results directly from the highly flexible chain architecture of PDMS (high diffusivity) and the tight polymer chain packing of Nafion® in its rubbery fluorocarbon and ionic sulfonic

acid domains (low diffusivity). In addition, but to a lesser extent, Nafion® also has lower gas solubility than conventional rubbery or glassy polymers, as discussed below.

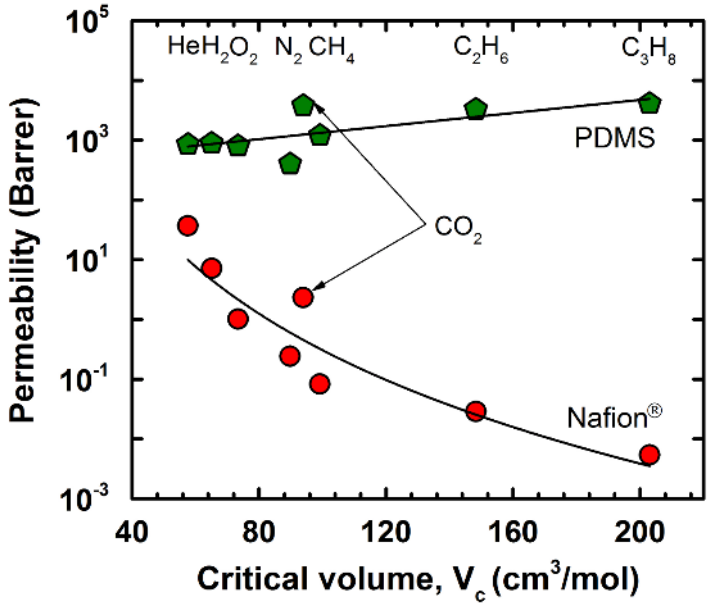


**Figure 3.** Gas permeability in dry Nafion® and rubbery PDMS[50] as a function of penetrant critical volume, $V_c$ at 35 °C.

***Gas Solubility and Diffusion Coefficients*.** The pure-gas solubility coefficients for He, $H_2$, $N_2$, $O_2$, $CO_2$, $CH_4$, $C_2H_6$, $C_3H_8$ and *n*-$C_4H_{10}$ are presented in Table 2. In this study, the gas solubilities were *directly* measured using barometric and gravimetric methods and are generally in good agreement. Previously reported solubility values by Chiou et al.[29] and Fan et al.[30] were calculated from the diffusion time-lag method, which is prone to errors especially for polymers with low gas solubility.[51] The solubility data for He and $H_2$, measured using the barometric method in this study agree reasonably well with the gravimetrically measured values reported by Smith et al.[34]

**Table 2. Gas Solubility Coefficients in Dry Nafion® at 2 atm and 35 °C.**

| | This work | | Reference | | |
|---|---|---|---|---|---|
| Gas | (Gravimetric) | (Barometric) | (Time lag)[a] | (Time lag)[b] | (Gravimetric)[c] |
| | Gas Solubility $S$ ($10^{-3}$ $cm^3$(STP)/$cm^3$·cmHg) | | | | |
| He | - | 0.52 | - | 0.28 | 0.49 |
| $H_2$ | - | 0.69 | 0.97 | 0.75 | 0.84 |
| $N_2$ | 1.3 | 1.3 | 1.5 | 0.97 | - |
| $O_2$ | 2.4 | 1.7 | 2.4 | 2.3 | - |
| $CH_4$ | 2.4 | 1.9 | 3.6 | 1.2 | - |
| $CO_2$ | 9.5 | 8.7 | 14.5 | 9.0 | - |
| $C_2H_6$ | 4.8 | 4.9 | - | - | - |
| $C_3H_8$ | 7.9 | 7.2 | - | - | - |
| $n$-$C_4H_{10}$ | 16.2[d] | 17.3[d] | - | - | - |

[a] Solubility coefficients calculated by S=P/D from permeability and diffusion time-lag method (1 atm; 35 °C).[29]

[b] Solubility coefficients calculated by S=P/D from permeability and diffusion time-lag method (4 atm; 30 °C).[30]

[c] Solubility coefficients measured directly by gravimetric method (10 atm; 35 °C).[34]

[d] Solubility coefficients measured at 1atm and 35 °C.

Sorption isotherms for He, $H_2$, $N_2$, $O_2$, $CO_2$, $CH_4$, and $C_2H_6$ in Nafion® measured at 35 °C using the barometric technique, shown in Figure 4(a) and (b), were linear up to 20 atm, following Henry's law. The isotherms of propane and *n*-butane in Figure 4(c) were convex to the pressure axis, which is well described by the Flory-Huggins theory for gas sorption in polymers. For comparison, isotherms determined by gravimetric sorption are in good agreement with those measured by the barometric sorption technique (Figure S1a-c).

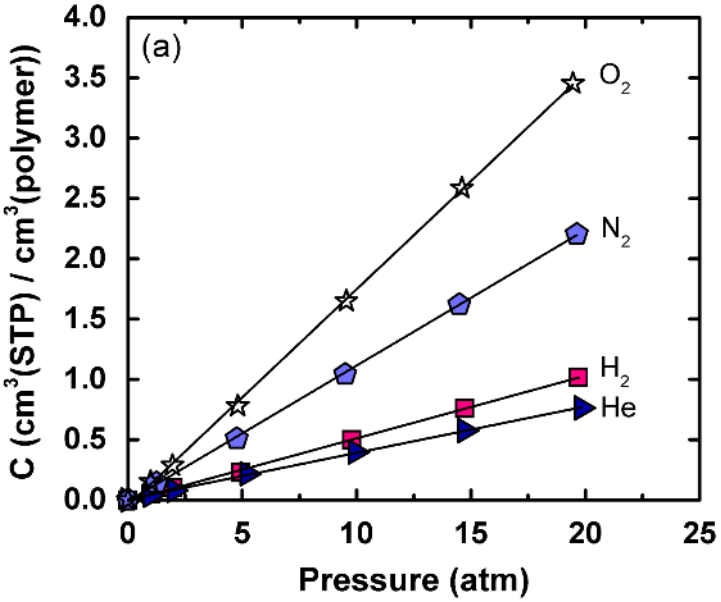
(a)
O2
N2
H2
He
C (cm3(STP) / cm3(polymer))
Pressure (atm)
0.0
0.5
1.0
1.5
2.0
2.5
3.0
3.5
4.0
0
5
10
15
20
25

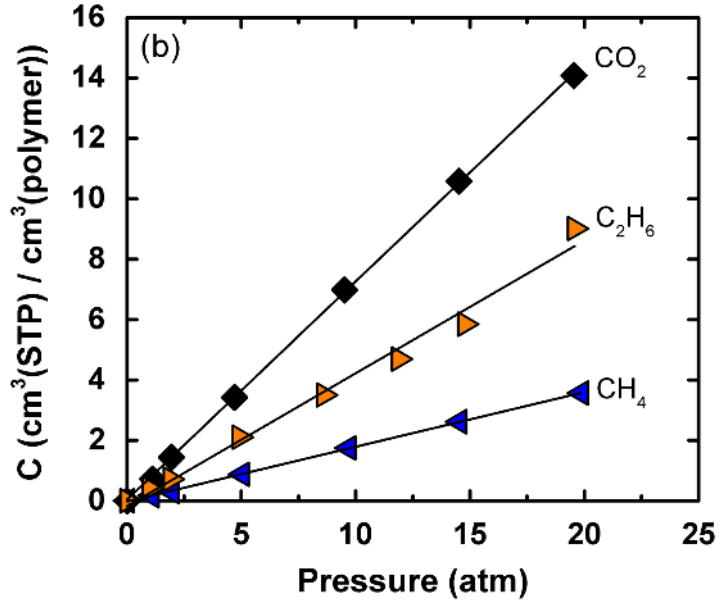
(b)
CO2
C2H6
CH4
C (cm3(STP) / cm3(polymer))
Pressure (atm)
0
2
4
6
8
10
12
14
16
0
5
10
15
20
25

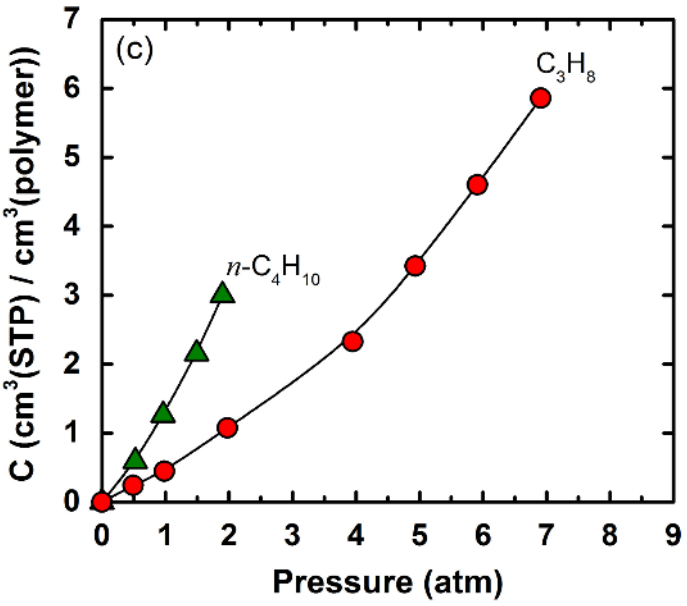


**Figure 4.** Sorption isotherms in dry Nafion® measured barometrically at 35 °C: (a) He, $H_2$, $N_2$, $O_2$; (b) $CO_2$, $CH_4$, $C_2H_6$; and (c) $C_3H_8$, $n$-$C_4H_{10}$.

The solubility of each penetrant in Nafion® as a function of pressure (Figure 5a) is compared with solubility values in rubbery PDMS (Figure 5b).[50] Both polymers show similar qualitative solubility trends. For low sorbing gases, such as $H_2$ and $N_2$, the absolute solubility values are similar in both polymers. However, for more highly sorbing hydrocarbon gases, such as $C_3H_8$, Nafion® exhibits up to 10-fold lower gas sorption than PDMS, most likely due to unfavorable fluorocarbon polymer-hydrocarbon gas interactions.[16]

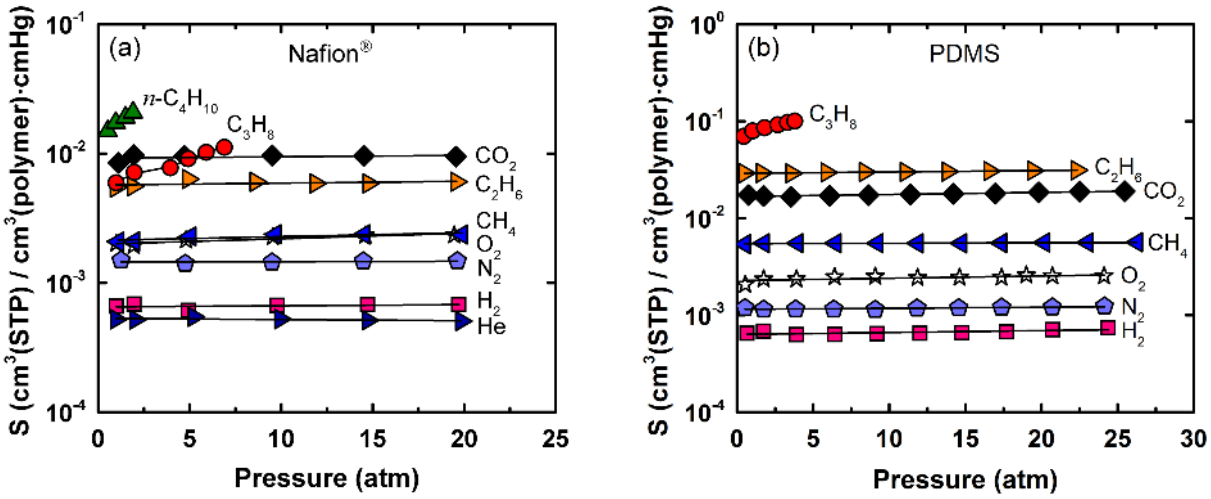


**Figure 5.** (a) Pressure dependent gas solubility in dry Nafion® measured barometrically at 35 °C for He, $H_2$, $N_2$, $O_2$, $CH_4$, $CO_2$, $C_2H_6$, $C_3H_8$, and *n*-$C_4H_{10}$ and (b) Pressure dependent solubility data for PDMS from reference [50] at 35 °C for $H_2$, $N_2$, $O_2$, $CH_4$, $CO_2$, $C_2H_6$, and $C_3H_8$.

Figure 6 presents gas solubility in Nafion® and a perfluorinated glassy polymer (Cytop®)[16] at 35 °C as a function of critical temperature. The solubility coefficients generally scale with gas condensability: He < $H_2$ < $N_2$ < $O_2$ ≈ $CH_4$ < $C_2H_6$ < $C_3H_8$. However, Nafion® and Cytop® have unusually high $CO_2$ solubility which deviates from the general trendline in Figure 6. Previous studies highlighted the unusual $CO_2$/perfluorocarbon interactions responsible for enhanced $CO_2$ solubility in perfluorinated liquids, which may also explain the observed higher solubility of $CO_2$ in Nafion® and Cytop®.[52,53] Additionally, it is well known that polymers containing polar moieties exhibit larger interaction with polar gases such as $CO_2$.[54] Thus, the interaction of quadrupolar $CO_2$ with the highly polar sulfonic acid group in Nafion® may have significant influence on its overall solubility.

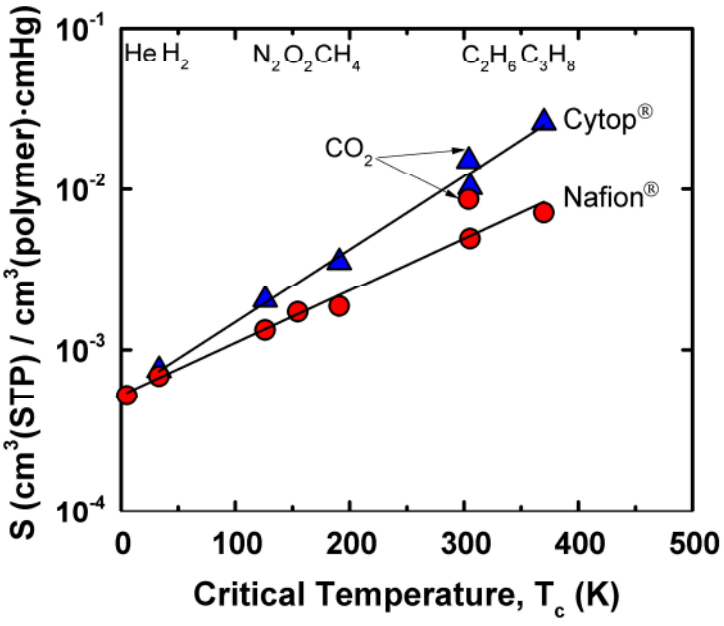


**Figure 6.** Solubility of gases in perfluorinated polymers at 35 °C: Nafion® and glassy Cytop®[9], as a function of critical temperature, $T_c$. The best-fit trendline through the experimental data for Nafion® is: $\ln S = -7.56 + 0.0078\ T_c$ [K].

Interestingly, the trend line through the solubility data of Nafion® differs from that of other perfluorinated polymers, such as Cytop®. This is primarily due to the extremely low hydrocarbon solubility observed in Nafion® with a slope value of 0.0078 $K^{-1}$ which is significantly lower than the general slope value for gas solubility in hydrocarbon- (0.017–0.019 $K^{-1}$)[36] and other perfluorocarbon-based (0.009–0.011 $K^{-1}$)[16] polymers. The deviation in slope for Nafion® compared to other perfluorinated polymers may be due to the hydrophilic sulfonic acid group that creates an additional unfavorable environment for sorption of the hydrocarbon penetrants in the polymer matrix. This lower solubility has significant implications for the separation

properties of gas pairs with large size differences: diffusivity selectivity to dominate overall permselectivity.

Pure-gas diffusion (D) coefficients in Nafion® calculated from the ratio of permeabilities and directly measured barometric sorption data at 2 atm and 35 °C are shown in Table 3. As expected, diffusivity decreases with increasing kinetic diameter (except for $CO_2$): He > $H_2$ > $O_2$ > $CO_2$ > $N_2$ > $CH_4$ > $C_2H_6$ > $C_3H_8$. The extent of these differences is extraordinary: the diffusivity of He is ~ 4 and 5 orders of magnitude higher than that of $C_2H_6$ and $C_3H_8$, respectively. This result highlights the exceptional molecular sieving properties of Nafion® for He/$C_{2+}$ hydrocarbons as well as $H_2$/$C_{2+}$ hydrocarbons and $CO_2$/$C_{2+}$ hydrocarbons, as shown in Table 4. Even similarly sized He ($d_k$= 2.60 Å) and $H_2$ ($d_k$= 2.89 Å) can efficiently be separated due to the strikingly high He/$H_2$ diffusivity selectivity of 6.8 and permselectivity of 5.2, which are the highest values for the He/$H_2$ pair of any known polymer reported to date. It is important to note that the high permselectivities of Nafion® do not solely result from its high diffusivity selectivities. The extremely low hydrocarbon gas solubilities lead to relatively small "inverse" solubility selectivity values for small, low sorbing gases over large, more condensable hydrocarbon gases (S(He) and S($H_2$) over $S_{hydrocarbons}$ <1).

**TABLE 3. Summary of Gas Diffusivity Coefficients in Dry Nafion® at 2 atm and 35 °C.**

| Gas | This study[a] | Reference [29][b] | Reference [30][c] |
|---|---|---|---|
| | Diffusivity ($10^{-8}$ $cm^2/s$) | | |
| He | 714 | - | 1076 |
| $H_2$ | 104 | 95.8 | 69 |
| $O_2$ | 5.9 | 4.57 | 3.19 |
| $CO_2$ | 2.7 | 1.68 | 1.56 |
| $N_2$ | 1.8 | 1.73 | 1.82 |
| $CH_4$ | 0.45 | 0.28 | 0.66 |
| $C_2H_6$ | 0.058 | - | - |
| $C_3H_8$ | 0.007 | - | - |

[a] Diffusion data were calculated from gas permeability and barometrically measured gas solubility values via solution-diffusion model (D=P/S).

[b] Determined by diffusion time-lag method at 35 °C.

[c] Determined by diffusion time-lag method at 30 °C.

**Table 4. Selectivity of Common Gas Pairs in Dry Nafion® at 2 atm and 35 °C.**

| Gas Pair | $P_a/P_b$ | $D_a/D_b$ | $S_a/S_b$ |
|---|---|---|---|
| $He/H_2$ | 5.2 | 6.9 | 0.75 |
| $He/CH_4$ | 445 | 1590 | 0.28 |
| $He/C_2H_6$ | 1275 | 12750 | 0.10 |
| $He/C_3H_8$ | 7400 | 102800 | 0.072 |
| $H_2/CH_4$ | 84 | 232 | 0.36 |
| $H_2/C_2H_6$ | 241 | 1790 | 0.135 |
| $H_2/C_3H_8$ | 1400 | 14580 | 0.096 |
| $CO_2/CH_4$ | 28 | 6 | 4.67 |
| $CO_2/C_2H_6$ | 79 | 47 | 1.68 |
| $CO_2/C_3H_8$ | 460 | 300 | 1.53 |

Note: Solubility data were calculated using barometric technique and diffusion data were obtained from D=P/S.

It is important to point out that this study was only focused on detailed evaluation of the intrinsic pure-gas transport properties of dry Nafion®. A water-swollen Nafion® membrane would certainly exhibit poorer gas separation performance due to loss of its size-sieving capabilities induced by enhanced chain mobility.

## CONCLUSIONS

Nafion® exhibits rubber-like gas solubility behavior at 35 °C as evidenced by linear sorption isotherms for low sorbing gases (e.g. $N_2$, $O_2$, $CH_4$ etc.) and convex sorption isotherms of more highly sorbing propane and *n*-butane. Hydrocarbon gas sorption in Nafion® is significantly lower compared to that observed in other perfluorinated glassy polymers; the best-fit trendline through the experimental gas sorption data as function of critical gas temperature for Nafion® is: $\ln S = -7.56 + 0.0078\ T_c$. WAXD data show that Nafion® contains tightly packed amorphous chain domains with sharp size-sieving regions separating gases based on their molecular sizes, which is more commonly observed in stiff-chain, low free volume glassy polymers. The strong size-sieving effect of dry Nafion® resulted in *extraordinarily* high permselectivity and was especially pronounced between small gases (He, $H_2$, $CO_2$) and large hydrocarbon gases ($C_{1+}$). This attribute can potentially be harnessed for dry feed steams for helium recovery and $CO_2$ removal in natural gas applications, and hydrogen recovery from refinery gas streams. However, It is important to point out that this study was only focused on detailed evaluation of the intrinsic pure-gas transport properties of *dry* Nafion®. A water-swollen Nafion® membrane would certainly exhibit

much poorer gas separation performance due to loss of its size-sieving capabilities induced by enhanced chain mobility, resulting in a significant loss in selectivity.[31]

## ASSOCIATED CONTENT

### Supporting Information

Gravimetric gas sorption isotherms are provided in the Supporting Information which is available free of charge on the ACS publication website.

## AUTHOR INFORMATION

### Corresponding Author

*Telephone: +966-12-808-2406 E-mail: ingo.pinnau@kaust.edu.sa (I.P.).

### Notes

The authors declare no competing financial interest.

## ACKNOWLEDGMENT

The authors acknowledge financial support of this work by KAUST funding for I.P. (BAS/1/1323-01-0).

## REFERENCES

1. Legault, A., Mainstreaming Efficient Industrial Separation Systems in *IEA OPEN Energy Technology Bulletin*, 2008.
2. Baker, R. W. *Ind. Eng. Chem. Res.* **2002**, 41, 1393-1411.
3. Bernardo, P.; Drioli, E.; Golemme, G. *Ind. Eng. Chem. Res.* **2009**, 48, 4638-4663.
4. Baker, R. W.; Lokhandwala, K. *Ind. Eng. Chem. Res.* **2008**, 47, 2109-2121.
5. Bernardo, P.; Drioli, E. *Petroleum Chem.* **2010,** 50, 271-282.

6. Yampolskii, Y. *Macromolecules* **2012**, 45, 3298-3311.

7. Baker, R. W.; Low, B. T. *Macromolecules* **2014**, 47, 6999-7013.

8. Sanders, D. F; Smith, Z. P.; Guo, R.; Robeson, L. M.; McGrath, J. E.; Paul, D. R.; Freeman, B. D. *Polymer* **2013**, 54, 4729-4761.

9. White, L. S.; Blinka, T. A.; Kloczewski, H. A.; Wang, I-F. *J. Membr. Sci.* **1995**, 103, 73-82.

10. Houde, A. Y.; Krishnakumar, B.; Charati, S. G.; Stern, S. A. *J. Appl. Polym. Sci.* **1996,** 62, 2181-2192.

11. Bos, A.; Pünt, I. G. M.; Wessling, M.; Strathmann. H. *J. Membr. Sci.* **1999**, 155, 67-78.

12. Wind, J. D.; Staudt-Bickel, C.; Paul, D. R.; Koros, W. J. *Macromolecules* **2003**, 36, 1882-1888.

13. Wind, J. D.; Paul, D. R.; Koros, W. J. *J. Membr. Sci.* **2004,** 228, 227-236.

14. Pinnau, I.; He, Z.; da Costa, A. R.; Amo, K. D.; Daniels, R. US Patent 6,361,582 B1, 2002.

15. Prabhakar, R. S.; Freeman, B. D.; Roman, I. *Macromolecules* **2004**, 37, 7888-7697.

16. Merkel, T. C.; Pinnau, I.; Prabhakar, R.; Freeman, B. D., Gas and Vapor Transport Properties of Perfluoropolymers. In *Materials Science of Membranes for Gas and Vapor Separation*; John Wiley & Sons, Ltd: 2006; pp 251-270.

17. He, Z.; Merkel, T. C.; Okamoto, Y.; Koike, Y. US Patent 8,828,121, 2014.

18. Okamoto, Y.; Zhang, H.; Mikes, F.; Koike, Y.; He, Z.; Merkel, T. C. *J. Membr. Sci*. **2014**, 471, 412-419.

19. Arcella, V.; Colaianna, P.; Maccone, P.; Sanguineti, A.; Gordano, A.; Clariza, G.; Drioli, E. *J. Membr. Sci*. **1999**, 163, 203-209.

20. Robeson, L. M., *J. Membr. Sci.* **2008**, 320, 390-400.

21. Steele, B. C. H.; Heinzel, A. *Nature* **2001,** 414, 345-352.

22. Mauritz, K. A.; Moore, R. B. *Chem. Rev.* **2004,** 104, 4535-4586.

23. Yeo, S. C.; Eisenberg, A. *J. Appl. Polym. Sci.* **1977,** 21, 875-898.

24. Gierke, T. D.; Hsu, W. Y., The Cluster-Network Model of Ion Clustering in Perfluorosulfonated Membranes. In *Perfluorinated Ionomer Membranes*; ACS Symposium Series 180, American Chemical Society: Washington DC, 1982; pp 283-307.

25. Corti, H. R.; Nores-Pondal, F.; Buera, M. P. *J. Power Sources* **2006,** 161, 799-805.

26. Sakai, T.; Takenaka, H.; Wakabayashi, N.; Kawami, Y.; Torikai, E. *J. Electrochem. Soc.* **1985**, 132, 1328-1332.

27. Wu, M. L. US Patent 4,666,468, 1987.
28. He, Y.; Cussler, E. L. *J. Membr. Sci.* **1992,** 68, 43-52.
29. Chiou, J. S.; Paul, D. R. *Ind. Eng. Chem. Res.* **1988,** 27, 2161-2164.
30. Fan, Y.; Tongren, D.; Cornelius, C. J. *Eur. Polym. J.* **2014,** 50, 271-278.
31. Catalano, J.; Myezwa, T.; De Angelis, M. G.; Giacinti Baschetti, M.; Sarti, G. C. *Int. J. Hydrogen Energy* **2012**, 37, 6308-6316.
32. Giacinti Baschetti, M.; Minelli, M.; Catalano, J.; Sarti, G. C. *Int. J. Hydrogen Energy* **2013**, 38, 11973-11982.
33. Osborn, S. J.; Hassan, M. K.; Divoux, G. M.; Rhoades, D. W.; Mauritz, K. A.; Moore, R. B. *Macromolecules* **2007,** 40, 3886-3890.
34. Smith, Z. P.; Tiwari, R. R.; Dose, M. E.; Gleason, K. L.; Murphy, T. M.; Sanders, D. F.; Gunawan, G.; Robeson, L. M.; Paul, D. R.; Freeman, B. D. *Macromolecules* **2014,** 47, 3170-3184.
35. Ghosal, K.; Freeman, B. D. *Polym. Adv. Technol.* **1994,** 5, 673-697.
36. Matteucci, S.; Yampolskii, Y.; Freeman, B. D.; Pinnau, I., Transport of Gases and Vapors in Glassy and Rubbery Polymers. In *Materials Science of Membranes for Gas and Vapor Separation*; John Wiley & Sons, Ltd: 2006; pp 1-47.
37. Barbari, T. A.; Conforti, R. M. *Polym. Adv. Technol.* **1994**, 5, 698-707.
38. Kamiya, Y.; Naito, Y.; Terada, K.; Mizoguchi, K.; Tsuboi, A. *Macromolecules* **2000,** 33, 3111-3119.
39. Vieth, W. R.; Howell, J. M.; Hsieh, J. H. *J. Membr. Sci.* **1976,** 1, 177-220.
40. Paul, D. R. *Berichte der Bunsengesellschaft für Phys. Chem.* **1979,** 83, 294-302.
41. van Amerongen, G. J. *J. Polym. Sci.* **1950**, 5, 307-332.
42. Takamatsu, T.; Eisenberg, A. *J. Appl. Polym. Sci.* **1979,** 24, 2221-2235.
43. Pye, D. G.; Hoehn, H. H.; Panar, M. *J. Appl. Polym. Sci.* **1976**, 20, 1921-1931
44. Koros, W. J.; Paul, D. R.; Rocha, A. A. *J. Polym. Sci. Part B: Polym. Phys.* **1976,** 14, 687-702.
45. Koros, W. J.; Paul, D. R. *J. Polym. Sci. Part B: Polym. Phys.* **1976,** 14, 1903-1907.
46. Laporta, M.; Pegorano, M.; Zanderighi, L. *Macromol. Mater. Eng*. **2000**, 282, 22-29.
47. van der Heijden, P. C.; Rubatat, L.; Diat, O. *Macromolecules* **2004**, 37, 5327-5336.
48. Hensley, J. E.; Way, J. D.; Dec, S. F.; Abney, K. D. *J. Membr. Sci.* **2007,** 298, 190-201.

49. Mohamed, H. F. M.; Kobayashi, Y.; Kuroda, C. Ohira, A. *Macromol. Chem. Phys.* **2011**, 212, 708-714.

50. Merkel, T. C.; Bondar, V. I.; Nagai, K.; Freeman, B. D.; Pinnau, I. *J. Polym. Sci., Part B: Polym. Phys.* **2000,** 38, 415-434.

51. Smith, Z. P.; Tiwari, R. R.; Murphy, T. M.; Sanders, D. F.; Gleason, K. L.; Paul, D. R.; Freeman, B. D. *Polymer* **2013,** 54, 3026-3037.

52. Evans, F. D.; Battino, R. *J. Chem. Thermodyn.* **1971**, *3*, 753.

53. Costa Gomes, M. F.; Padua, A. A. H. *J. Phys. Chem. B* **2003***,* 107, 14020-14024.

54. Kazarian, S. G.; Vincent, M. F.; Bright, F. V.; Liotta, C. L.; Eckert, C. A. *JACS* **1996,** 118, 1729-1736.

Table of Contents Graphic

# Gas Sorption, Diffusion and Permeation in Nafion®

Mohsin Mukaddam, Eric Litwiller, Ingo Pinnau*